ROYAL SOCIETY
OF CHEMISTRY

PAPER

Check for updates

A highly effective curcumin analogue as "naked eye" colorimetric and fluorescent sensor for sensitive and selective detection of Hg^{2+} ions and its application on test strips and real sample analysis†

Ramesh D. K.[ab] and Prasad Pralhad Pujar [ID] *[ab]

A thiophene appended curcumin-based colorimetric and fluorescent receptor (TAA) for selective recognition of Hg^{2+} ions was synthesized and characterized using ^{1}H NMR, ^{13}C NMR and LC-MS spectroscopic techniques. TAA facilitates detection of Hg^{2+} by a "naked-eye" color change from yellow to colorless in visible light, and fluorescence 'turn-off' in UV light (365 nm). The observed fluorescence quenching is due to the chelation-enhanced fluorescence quenching (CHEQ). TAA exhibited excellent selectivity and sensitivity toward Hg^{2+} ions, even in the presence of competing cations. The binding constant (K_a) for Hg^{2+} ions was found to be 3.4×10^5 M^{-1}, indicating a strong binding affinity. The binding mechanism was elucidated using DFT calculations and supported by LC-MS and FT-IR studies. TAA forms a 1:1 complex with Hg^{2+} ions, as confirmed by Job's plot analysis. Additionally, the colorimetric limit of detection was found to be 0.67 μM, while the fluorometric limit of detection was found to be 0.24 μM, which demonstrates the high sensitivity of TAA towards Hg^{2+}. Furthermore, TAA probe exhibited successful detection of Hg^{2+} ions in real water samples. Also, it can serve as an effective on-site detection tool for mercury ions by a simple test strip method that requires no additional instrumentation.

1 Introduction

The environment has been polluted by both biological and non-biological sources, such as harmful bacteria, sewage effluents, animal waste, heavy metals, and both industrial and municipal waste.[1] Due to the rapid pace of industrialisation, heavy metal pollution has become a major global environmental concern. Common heavy metals such as mercury (Hg^{2+}), arsenic (As^{3+}), lead (Pb^{2+}), cobalt (Co^{2+}), cadmium (Cd^{2+}), nickel (Ni^{2+}), and chromium (Cr^{3+}) are known for their high toxicity, persistence in the environment, resistance to degradation, and water solubility. Exposure to such toxic metals above permissible levels can pose serious risks not only to human health, but also to aquatic and terrestrial living beings.[2–4]

Particularly, the extensive use of mercury ions (Hg^{2+}) in batteries, paints, and other electronic goods has resulted in considerable environmental damage and poses a serious threat

^{a}Department of Chemistry, Christ University, Hosur Road, Bangalore, Karnataka 560029, India. E-mail: prasad.pujar@christuniversity.in

^{b}Centre for Renewable Energy and Environmental Sustainability, Christ University, Bangalore 560029, India

† Electronic supplementary information (ESI) available. See DOI: https://doi.org/10.1039/d5ra03656a

to both human health and natural systems.[5] High intake of Hg^{2+} causes serious threats to human health as it can penetrate biological membranes, leading to severe damage to the blood capillaries, brain, kidneys, nervous system, and digestive system. It is a known fact that the accumulation of Hg^{2+} in human bodies can occur through food and drinks, which leads to the importance of detecting Hg^{2+} at the source, especially aqueous level.[6–8] The World Health Organization (WHO) and other national authorities have stated that mercury is recognized as one of the top ten most dangerous chemicals causing serious risks to human health. It is difficult to detect heavy metal ions such as Hg^{2+} in an aqueous environment due to the effective hydration and high stabilization.[9] Hence, there is a strong demand for the development of efficient, rapid, and on-site methods for the detection of Hg^{2+} in aqueous environments.[10]

Various methods are employed for the detection of metal ions, ranging from traditional physicochemical approaches to advanced analytical techniques such as atomic absorption spectrometry (AAS), atomic fluorescence spectrometry (AFS),[11] mass spectrometry,[12] liquid chromatography, and gas chromatography.[13] But these analysis methods are expensive, time-consuming and less sensitive and hence, the development of optical sensors with rapid, low-cost, simple, and sensitive metal

ion detection is the need of present world.[14] In order to overcome this, optical sensors like UV-vis and fluorescence sensors have attracted great attention and are well-suited for Hg^{2+} sensing.[15–20] This method is rapid, sensitive, low-cost and selective as well. Using organic molecules in such a process will provide an environmentally friendly approach. Several fluorophores with different moieties such as fluorescein,[21] rhodamine,[22] benzimidazole,[23] anthracene,[24] pyrene,[25] coumarin,[26] quercetin,[27] nanoparticles[28] and fluorescent nanofibers[29] have been reported for the detection of Hg^{2+}. Among these, one such fluorophore is curcumin, which is a fluorescent molecule having a large planar structure with more π-conjugation that could be used as a fluorophore for metal ion detection.

Curcumin, a natural yellow pigment isolated from dried turmeric rhizomes, exhibits low cytotoxicity, excellent photostability, and is a popular medicinal herb. Also, curcumin has been popular for its biological activities, such as anti-inflammatory, anti-aging, anti-microbial, antiproliferative, anti-cancer, radioprotective, neuroprotective, and cardioprotective properties.[30–33] Apart from its pharmacological nature, curcumin has been used in food and food packaging[34] and also as a fluorescent probe in biomedical applications.[35] Curcumin and its derivatives have a large conjugate structure, which aids in the electron delocalization, enabling them to emit long-wavelength fluorescence. It contains 1,3-diketones with keto–enol isomerization, and is a chelating site for various toxic cations and anions based on the Intramolecular charge transfer (ICT) mechanism.[36] Due to this, curcumin has great significance in chelation treatment and heavy-metal intoxication. Although several studies reported curcumin-based sensors (Table S1†), there remains great potential for further development by modifying its core structure or employing its analogues in various sensing applications.

Thiophenes are highly reactive organic building blocks that could be used in the field of sensors as a functional group, because of their excellent chemical stability, high carrier mobility, and unique photo-physical properties.[37] Curcumin analogue with a thiophene moiety could enhance the fluorescence emission wavelength. Motivated by the above-mentioned characteristics, we developed a thiophene-based curcumin analogue as an Hg^{2+} probe for selective and sensitive detection with a low limit of detection in aqueous medium. This work presents a simple and facile approach for Hg^{2+} detection and provides rapid, non-toxic, naked eye detection.

2 Experimental

2.1 Materials and methods

The synthesis chemicals and solvents were purchased from Avra Chemicals and SD Fine and used without further purification. The NMR spectra were recorded using a Bruker 400 MHz spectrometer using $CDCl_3$ as the solvent, and tetramethylsaline (TMS) as an internal standard. LC-MS data was recorded using an ESI ionization in the LCMS-8060NX instrument from Shimadzu. The Shimadzu IR Spirit spectrophotometer was used to record Infrared spectra. Absorption measurements were carried out with a Shimadzu UV-1800, and fluorescence measurements
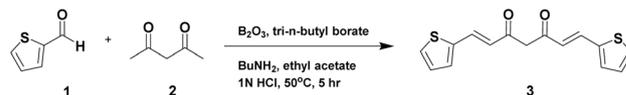
Scheme 1 Synthesis of (1E,6E)-1,7-di(thiophen-2-yl)hepta-1,6-diene-3,5-dione (TAA).

were carried out with a RF-6000 Spectrofluorophotometer. Analytical thin-layer chromatography (TLC) was performed on pre-coated plates (Merck, silica gel 60F254).

2.2 General procedure of synthesis of TAA

The preparation of the Curcumin analogue was carried out according to the known method (AN Nurfina et al.[38]). The reaction was carried out using thiophene-2-carboxaldehyde and acetylacetone as the starting materials. The acetylacetone (0.5 equivalent) was added to the solution of boric anhydride (0.5 equivalent) in ethyl acetate (8 mL). Thiophene-2-carboxaldehyde (1 equivalent) and tri-n-butyl borate (0.75 equivalent) were added to this solution and stirred for 10 minutes at 50 °C. Furthermore, n-butylamine was added dropwise for a prolonged period of 5 minutes, and the reaction was continued for 5 hours at 50 °C. Hydrochloric acid (1 N) was added, and the reaction was stirred for another 60 minutes (Scheme 1). The reaction was monitored using thin-layer chromatography (TLC), and a yellow-coloured fluorescent spot was observed indicating completion of the reaction. The reaction was worked up as explained in the reported method to obtain yellow solid of curcumin analogue TAA with 82% yield.

2.2.1 Experimental procedure and analytical data of the curcumin analogue (3)

2.2.1.1 Synthesis of (1E,6E)-1,7-di(thiophen-2-yl)hepta-1,6-diene-3,5-dione (TAA). The reaction was carried out by treating thiophene-2-carbaldehyde **1** (200 mg, 1 eq.) and acetyl acetone **2** (89 mg, 0.5 eq.) in presence of boric anhydride, tri-butyl borate, and n-butyl amine as a base in ethyl acetate to obtain the desired (1E,6E)-1,7-di(thiophen-2-yl)hepta-1,6-diene-3,5-dione **3** with 82% yield.

(1E,6E)-1,7-di(thiophen-2-yl)hepta-1,6-diene-3,5-dione (TAA, Scheme 1): The compound obtained is a yellow solid. Yield: 421.7 mg (82%); ^{1}H NMR (400 MHz, $CDCl_3$) δ: 7.78 (d, $J = 10$ Hz, 1H), 7.38 (d, $J = 2.8$ Hz, 1H), 7.26 (d, $J = 2.4$ Hz, 1H), 7.067 (t, 1H), 6.41 (d, $J = 10.4$ Hz, 1H), 5.78 (s, 1H).

^{13}C NMR (400 MHz, DMSO): δ 183.00, 140.30, 133.72, 132.55, 130.55, 129.24, 123.18, 101.99. Mass spectrometry: LCMS (ESI) m/z: calculated for $C_{15}H_{12}O_2S_2 = 288.38$, found = 289.

2.3 Photophysical properties

Ten solvents with different polarities i.e. methanol, ethanol, DMSO, DMF, DCM, acetonitrile, tetrahydrofuran, ethyl acetate, toluene and hexane were employed to investigate the excitation and emission behaviour of the synthesized TAA. For this purpose, the absorbance and fluorescence emission spectra of the compound were measured in various solvents using 25 μM solutions of TAA.

2.4 General procedure for spectroscopic measurements

A Stock solution of the probe TAA (1 mM) was prepared using HPLC grade CH_3CN. The stock solutions of other various cations (1 mM) used in the study were prepared by dissolving the following compounds in distilled water: $Al(NO_3)_3$, $BaCl_2$, $Cd(NO_3)_2$, $CoSO_4$, $CrCl_2$, $AgNO_3$, $Fe(NO_3)_3$, $FeCl_2$, $HgCl_2$, Li_2SO_4, $MgCl_2$, $MnSO_4$, $NiSO_4$, $Pb(NO_3)_2$, $ZnSO_4$. The other test solutions of anions were prepared using tetra butyl ammonium salts of I^-, Br^-, ClO_4^-; sodium salts of $S_2O_3^{2-}$, F^-, Cl^-, NO_3^-, N_3^- and ammonium salt of acetate. All spectroscopic measurements were performed at room temperature using a CH_3CN/H_2O mixture (v/v = 1:1). A 25 µM and 50 µM solution of the probe TAA and analytes were used for binding studies. The excitation and emission slit widths were set to 5 nm and 5 nm, respectively, for all measurements.

2.5 Stoichiometry and binding constant calculation

The stoichiometry of the probe TAA and Hg^{2+} was analysed by performing a Job's plot. Stock solutions of the probe TAA and Hg^{2+} were made at a concentration of 25 µM and 50 µM, respectively. The final volume was kept to be 3 ml, and varying volumes of Hg^{2+} (0.3–2.7 ml) and the probe TAA (2.7–0.3 ml) were mixed in a quartz cuvette. A Job's plot was then constructed by plotting the mole fraction against absorbance to determine the mole fraction at which complex formation was maximal.

The binding constant of the complex was evaluated using the Benesi–Hildebrand (B–H) plot. The following equation was used to determine the binding constant.

$$\frac{1}{A_0 - A} = \frac{1}{K_a(A_{max} - A)C} + \frac{1}{(A_{max} - A)} \quad (1)$$

where A_0 is the absorbance in the absence of Hg^{2+}, A is the absorbance in the presence of Hg^{2+}, C denotes the concentration of Hg^{2+} added during the titration, and A_{max} represents the maximum absorbance recorded throughout the experiment.

By absorption and fluorescence titration plot, the limit of detection (LOD) of Hg^{2+} was measured. The standard deviation was achieved by the absorption and fluorescence spectra of the probe, which were calculated from repeated measurements. To attain the slope, the calibration plot between the absorption and fluorescence intensities and the concentration of the analyte (Hg^{2+}) was calculated using the following equation:

$$\text{The limit of detection} = \frac{3\sigma}{K} \quad (2)$$

where σ is the standard deviation of the probe, K is the slope value from the linear calibration plot.

2.6 pH study

To evaluate the influence of pH on the fluorescence sensing performance of probe TAA towards Hg^{2+}, solutions of TAA (25 µM) were prepared with and without Hg^{2+} (50 µM) across a pH range of 2–12, using 1 N HCl and 1 N NaOH. The fluorescence spectra of these solutions were then recorded.

2.7 DFT calculations

To validate complex formation, the Gaussian 09 software was used to carry out theoretical calculations. Using the B3LYP/6-311G++ (d, p) basis set, the ground and excited state geometries of the probe TAA were optimized. Further, a B3LYP/LANL2DZ basis set was used to improve the geometry of the TAA-Hg^{2+} complex.

2.8 Real sample analysis

In order to analyse the ability of the probe TAA to detect Hg^{2+} in the environmental samples, real water analysis was carried out. Different water samples, like river water, lake water, pond water, tap water and drinking water samples, were collected and filtered through Whatman filter paper. In the end, the Hg^{2+} solution was injected into the samples and analyzed.

2.9 Fabrication of test paper strip

The square strips of Whatman filter paper were dipped in the solution of TAA and air dried for 10 minutes. Further, these strips were again soaked in a solution of different metal ions for 10 minutes and dried. Then these strips were examined under visible and UV light (365 nm).

3 Results and discussion

3.1 Design and synthesis

In this research, a fluorescent and colorimetric sensor based on curcumin was developed to detect Hg^{2+} ions. Curcumin generally exhibits fluorescence due to its extended π-electrons conjugation, which allows for electron delocalization from one end to the other end of the molecule. Additionally, it can undergo keto–enol tautomerism, contributing to its unique photophysical properties. On the other hand, with the α,β-unsaturated-diketone component as the recognition site for the analyte, the design of a thiophene moiety to the α,β-unsaturated-diketone moiety facilitates the chelation-enhanced fluorescence quenching (CHEQ) process with Hg^{2+} ions. As shown in (Scheme 1), the synthesis of the probe TAA was performed by reacting thiophene-2-carbaldehyde with acetylacetone in a 2:1 ratio in ethyl acetate *via* a condensation reaction.

Table 1 Absorption and emission properties of TAA in different solvents

Solvents	$\lambda_{(ex)}$ nm	$\lambda_{(em)}$ nm	Stokes shift (cm^{-1})
Methanol	428	525	4317
Ethanol	418	521	4730
DMSO	438	514	3376
DMF	436	515	3518
DCM	434	537	4420
Acetonitrile	417	522	4823
Tetrahydrofuran	416	516	4659
Ethyl acetate	445	504	2630
Toluene	418	517	4581
Hexane	410	509	4744

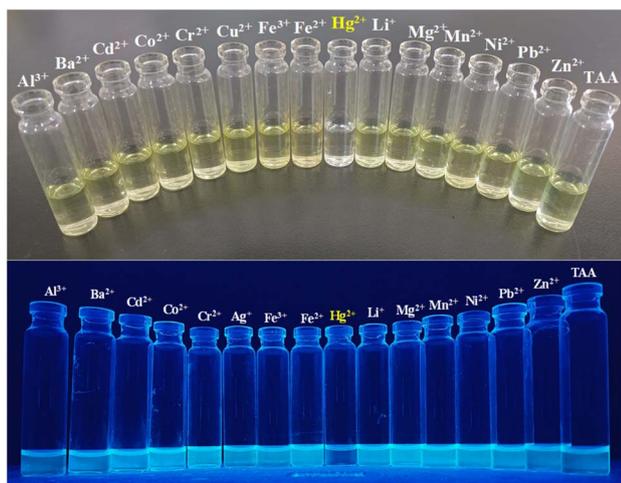**Fig. 1** Visual change of TAA in comparison with other metal ions: visible light (upper image), UV-light (365 nm) (lower image).
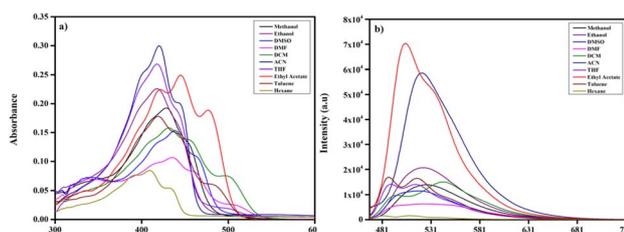

Fig. 2 (a) UV-vis absorption and (b) fluorescence spectra of TAA (25 μM) in different solvents.

The product was obtained in good yield (82%). The synthesized TAA was characterized by ^{1}H NMR, ^{13}C NMR, LC-MS techniques.

3.2 Photophysical properties of prepared TAA

The screening of the synthesized TAA molecule was done in order to study the Hg^{2+} ion sensing. Based on the position of the excitation and emission peak and also the Stokes shift values of

TAA (25 μM) in ten different solvents of varying polarity (Table 1), the highest Stokes shift with better excitation and emission spectra was chosen for the absorption–emission titrations of the Hg^{2+} ion detection study. The excitation and emission peaks were found to be at 417 nm and 522 nm in acetonitrile (CH_3CN), which showed a better and broader intensity peak compared to other solvents with a better Stokes shift value (Fig. 1). Thus, acetonitrile was used as the solvent for TAA in further analysis.

3.3 Visual detection of TAA in response to various metal ions

Colorimetric tests as well as fluorescence change of the probe TAA were performed using a range of metal ions including Al^{3+}, Ba^{2+}, Cd^{2+}, Co^{2+}, Cr^{2+}, Ag^+, Fe^{3+}, Fe^{2+}, Hg^{2+}, Li^+, Mg^{2+}, Mn^{2+}, Ni^{2+}, Pb^{2+} and Zn^{2+}. The probe TAA displayed a distinct yellow color in CH_3CN. Upon the addition of these metal ions to a CH_3CN/H_2O mixture (v/v = 1 : 1) there was no significant color change observed, except in the case of Hg^{2+} ions (Fig. 2), which was colorless solution. The probe TAA also showed bright yellow fluorescence under UV light (365 nm) in CH_3CN. Upon addition of Hg^{2+} ion the fluorescence was completely quenched, but there was no significant impact on the fluorescence intensity with the addition of other metal ions. This indicates that the probe TAA exhibits high sensitivity and selectivity specifically toward Hg^{2+}. The decolorisation and fluorescence quenching observed upon Hg^{2+} binding is attributed to the preferential coordination of the Hg^{2+} ion with the di-ketone moiety of the sensor, leading to a highly selective detection response.

3.4 Spectroscopic behaviour of TAA upon interaction with Hg^{2+}

The optical properties of the TAA probe (25 μM) in the absence and presence of Hg^{2+} (50 μM) were investigated using UV-vis absorption and fluorescence spectroscopy. The TAA probe exhibited a prominent absorption band at 417 nm. Upon addition of 50 μM of Hg^{2+} ion, the absorbance at 417 nm decreased, while a new absorption band emerged at 340 nm (hypsochromic shift). This was accompanied by a visible color change from yellow to colorless solution. This indicates the potential of TAA for colorimetric detection of Hg^{2+}. Further,
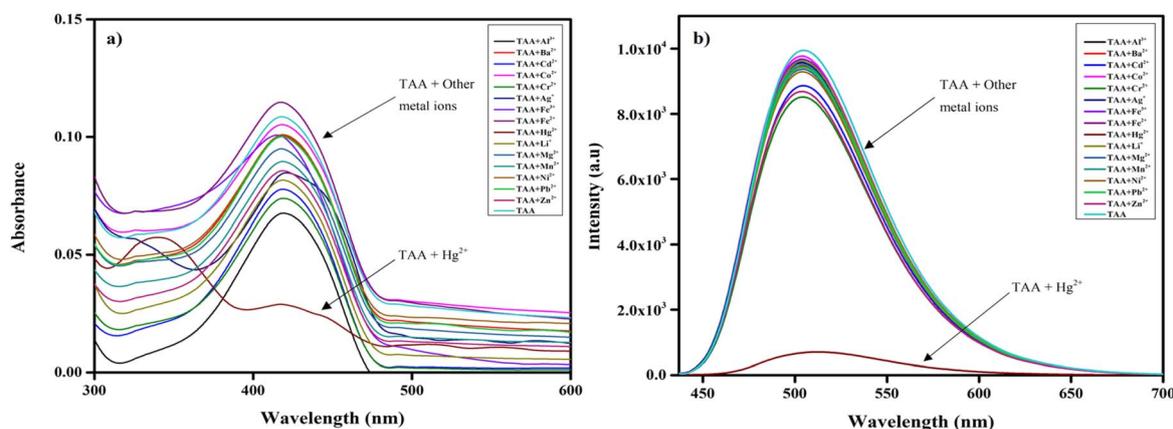

Fig. 3 (a) UV-vis and (b) fluorescence spectra of TAA (25 μM) with various metal ions (50 μM) in CH_3CN/H_2O (v/v: 1/1).
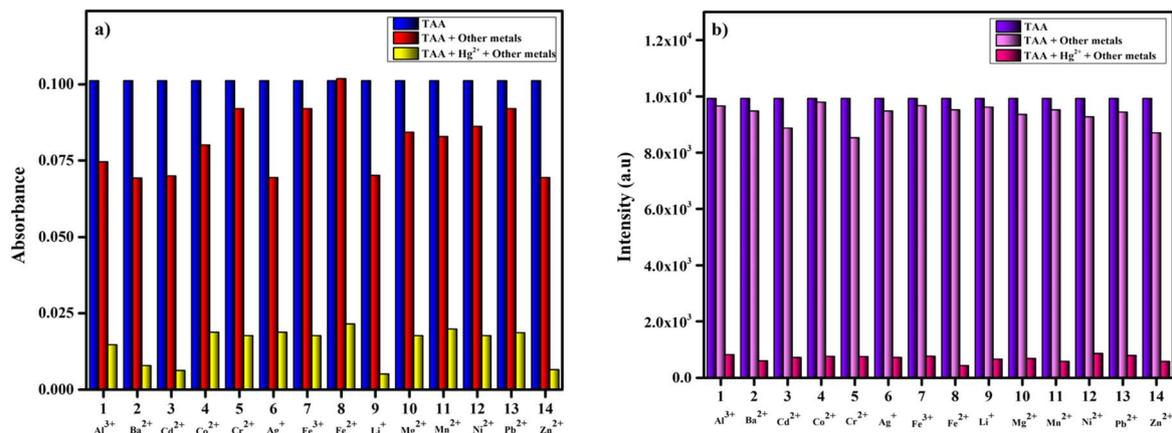
Fig. 4 Competitive study of TAA (25 µM) with Hg^{2+} upon addition of other interfering metal ions (50 µM): (a) absorption studies, (b) emission studies.

fluorescence studies revealed strong emission intensity at 505 nm for the TAA probe in H_2O (v/v = 1 : 1). After introducing Hg^{2+} (v/v = 1 : 1), the fluorescence intensity significantly decreased due to chelation-enhanced fluorescence quenching (CHEQ) (Fig. S4†). The transfer of electrons from the probe to the analyte is attributed to the initiation of the photo-induced electron transfer (PET) process *i.e.* complexation of probe with Hg^{2+} leads to the non-radioactive decay pathway which in turn results in the quenching of the intrinsic fluorescence of TAA, thereby functioning as a turn-off fluorescence probe for the selective detection of Hg^{2+} ions.[39]

3.5 Selectivity studies of TAA

The selectivity of the TAA probe for the detection of Hg^{2+} in comparison with other metals was studies. The absorption and fluorescence spectra of the TAA probe after the addition of different analytes, including Al^{3+}, Ba^{2+}, Cd^{2+}, Co^{2+}, Cr^{2+}, Ag^+, Fe^{3+}, Fe^{2+}, Hg^{2+}, Li^+, Mg^{2+}, Mn^{2+}, Ni^{2+}, Pb^{2+} and Zn^{2+} were measured (Fig. 3a and b). After adding these analytes, no significant change was observed in the absorption and emission intensities, except Hg^{2+}. The absorption peak blue-shifted to 340 nm, and the fluorescence intensity of the TAA probe was
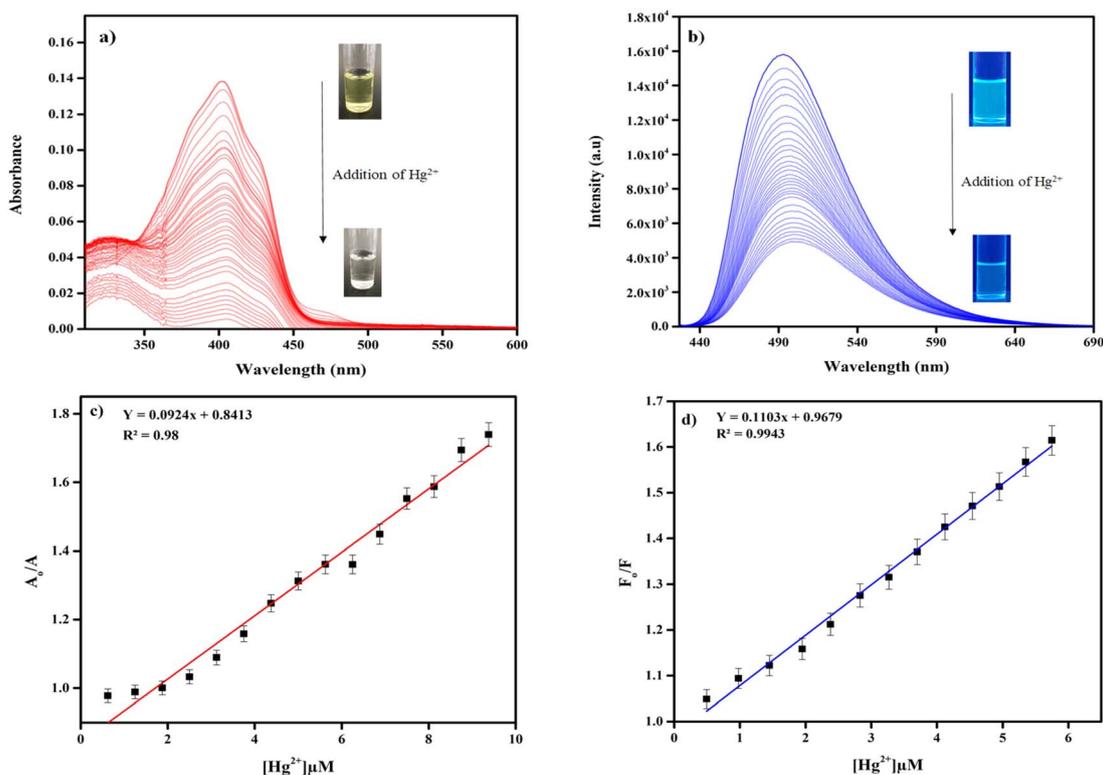

Fig. 5 (a) UV-vis and (b) fluorescence titration plot of TAA (25 µM) upon addition of Hg^{2+} (50 µM), detection limit of TAA by (c) UV-vis spectroscopy, (d) fluorescence spectroscopy.
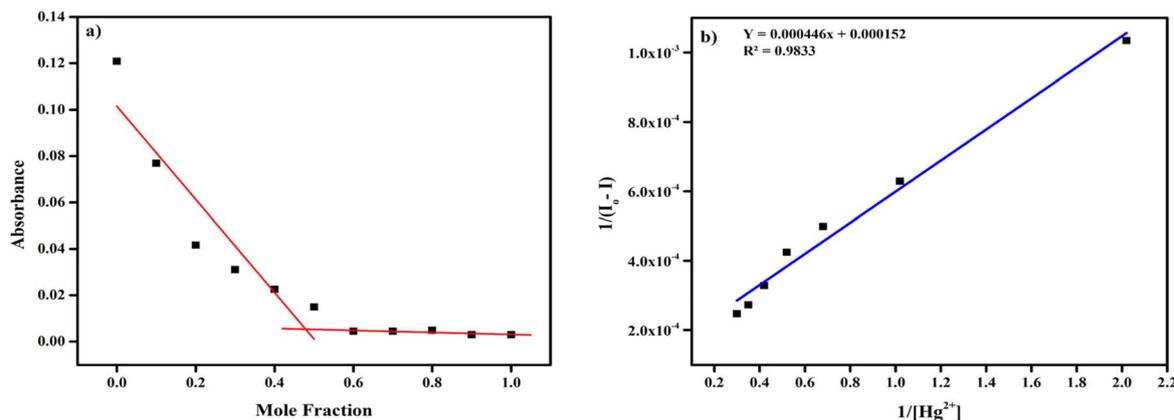
Fig. 6 (a) Job's plot of TAA (25 μM) for Hg^{2+} (50 μM), (b) Benesi−Hildebrand (B−H) plot of TAA (25 μM) for Hg^{2+} (50 μM).

sharply quenched after its reaction with Hg^{2+}. These data demonstrated the high selectivity of the TAA probe to Hg^{2+}. We further extended the UV-Vis and fluorescence studies of TAA by evaluating its response in the presence of various competing anions including Br^-, CH_3COO^-, Cl^-, ClO_4^-, F^-, I^-, N_3^-, NO_3^- and $S_2O_3^{2-}$. As shown in Fig. S6,† the sensor exhibited no significant interference from any of these anions.

3.6 Anti-interference studies of TAA

To evaluate the selectivity and anti-interference capability of TAA for practical applications, a competitive study was conducted in the presence of various potential interfering metal

Fig. 7 Time evolution of TAA (25 μM) towards Hg^{2+} (50 μM), (a) UV-vis spectroscopy, (b) fluorescence spectroscopy.

ions, including Al^{3+}, Ba^{2+}, Cd^{2+}, Co^{2+}, Cr^{2+}, Ag^+, Fe^{3+}, Fe^{2+}, Hg^{2+}, Li^+, Mg^{2+}, Mn^{2+}, Ni^{2+}, Pb^{2+} and Zn^{2+}. Initially, absorption studies at 417 nm were carried out using solutions containing 25 μM of TAA along with 50 μM of various other interfering metal ions, which displayed no significant change in absorption in comparison with TAA. When Hg^{2+} was introduced with other metal ions, decrease in the absorbance of the TAA-Hg^{2+} complex was observed (Fig. 4a). Similarly, in fluorescence spectroscopy (Fig. 4b), TAA solutions with competing ions exhibit significant fluorescence at 505 nm, which are quenched after the addition of Hg^{2+}. These findings confirm the outstanding selectivity of TAA for Hg^{2+} detection, even in complex environments. As Hg^{2+} is a soft metal, the selective affinity of Hg^{2+} towards TAA over other competing metal ions may be attributed to its strong preference for binding with soft bases, particularly favoring sulfur-containing ligands. In this study, the presence of a sulfur atom in the ligand likely plays a crucial role in facilitating the specific interaction with Hg^{2+} over other metal ions.[40]

3.7 Sensitivity studies of TAA

To investigate the sensitivity of TAA (25 μM) towards Hg^{2+} (50 μM) ions, UV-vis and fluorescence titration experiments were conducted in a CH_3CN/H_2O (v/v, 1 : 1) medium. Upon incremental addition of Hg^{2+} ions, decrease in absorption and fluorescence intensity at 417 nm and 505 nm was observed (Fig. 5a and b). This indicates that TAA exhibits a specific response towards Hg^{2+} due to complex formation.

Furthermore, using UV-vis and fluorescence titration curves the limit of detection (LOD) for Hg^{2+} ions was calculated (using eqn (2)) and were determined to be 0.67 μM and 0.24 μM, respectively (Fig. 5c and d), indicating the use of TAA in simulated water samples. The LOD value was found to be quite low compared to the recent sensor reports (Table 3). The colorimetric and fluorometric linear detection range was found within 0–10 μM ($R = 0.98$) and 0–6μM ($R = 0.9943$), respectively. The fluorescence quantum yield was determined using quinine sulphate as a reference standard, which has a known quantum yield (Φ_R) of 0.54 in distilled water. The calculated quantum
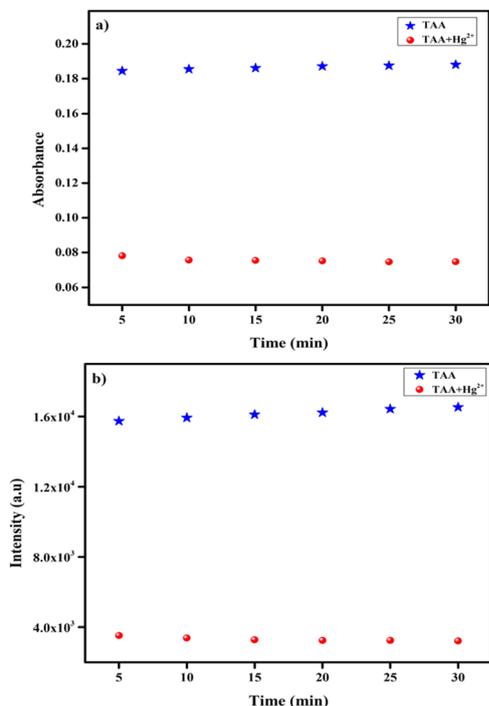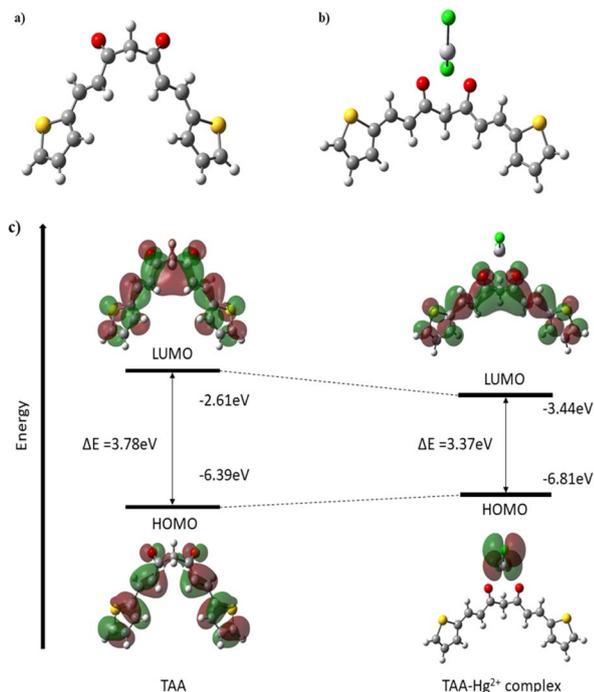
Paper

Fig. 8 Geometry optimized structures of: (a) TAA, (b) TAA-Hg^{2+} complex, (c) frontier molecular orbital with energy difference of TAA and TAA-Hg^{2+} complex.
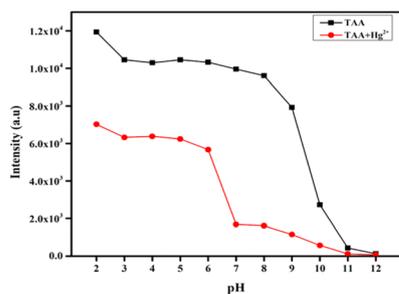

Fig. 9 Effect of pH on TAA (25 μM) and TAA-Hg^{2+} in fluorescence spectroscopy.

yield values were 0.0229 for TAA and 0.0029 for the TAA-Hg^{2+} complex. The photo image of colorimetric linear detection from yellow to colorless is been noticed proportional to the concentration of Hg^{2+} (Fig. S8†). Therefore, TAA demonstrates strong potential as a visual colorimetric probe for Hg^{2+} detection under environmental conditions.

3.8 Binding stoichiometry ratio analysis of TAA with Hg^{2+}

To gain deeper insight into the binding affinity of TAA towards Hg^{2+}, the stoichiometry and binding constant were further evaluated using Job's and Benesi–Hildebrand (B–H) plots. In Job's plot, the [TAA]/([TAA] + [Hg^{2+}]) = 0.5 mole fraction, indicates the stoichiometry ratio of TAA to Hg^{2+} is 1 : 1 (Fig. 6a). Binding affinity was further supported by the linearity of the B–H plot (Fig. 6b), which yielded a high correlation coefficient
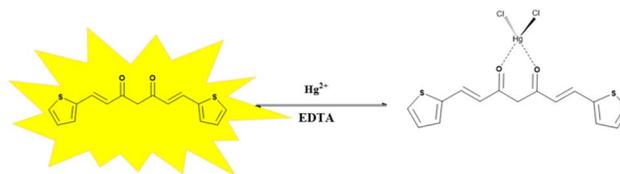
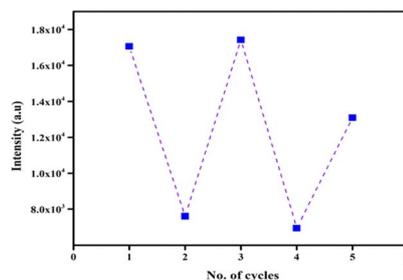Scheme 2 Probable binding mode in the solution phase.

Fig. 10 Reversibility cycle of TAA (25 μM) with EDTA (50 μM).

$(R^2 = 0.9833)$. The binding constant (K_a) was calculated to be 3.4 $\times 10^5$ M^{-1}. Upon complexation, the core moiety gets the charge density, which in turn induces a chelation-enhanced fluorescence quenching (CHEQ) effect. Additionally, a stable photoinduced electron transfer (PET) mechanism is triggered.[41]

In order to know the binding mechanism, infrared (IR) spectroscopy was performed. The IR spectrum showed C=O stretching vibration at 1625 cm^{-1} in the free ligand. But, the IR spectrum of the complex revealed that there was no C=O stretching vibration (Fig. S5†). These spectral changes provide strong evidence of Hg^{2+} coordination through the di-ketone moiety (–C=O) of the ligand. To further demonstrate the binding mechanism, mass spectrum of TAA-Hg^{2+} complex was taken, that indicates a peak at $m/z = 568$ was assignable to [TAA + Hg^{2+} + Cl$_2^-$ + $\frac{1}{2}$H$_2$O] (Fig. S7†).
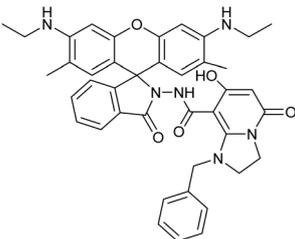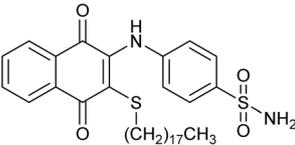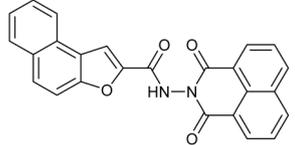
3.9 Time response of TAA towards Hg^{2+}

The time-dependent behavior of probe TAA (25 μM) towards Hg^{2+} (50 μM) was performed, the absorption and the emission intensities of TAA at 417 nm and 505 nm remained nearly constant for up to 30 minutes. Furthermore, a rapid response time of approximately 4–5 seconds was observed for the interaction between the TAA-Hg^{2+} complex, the absorption and emission peaks appeared when the recognition process

Table 2 Determination of Hg^{2+} in different real water samples

Samples	Hg^{2+} spiked (μM)	Hg^{2+} found (μM)	Recovery (%)
River water	5.00	5.10	102.0
Lake water	5.00	5.06	101.2
Pond water	5.00	5.03	100.6
Tap water	5.00	4.98	99.6
Drinking water	5.00	4.99	99.8

Table 3 Comparison of previously reported Hg^{2+} sensors with the present work

S no.	Ligand	Sensing method	Probe type	LOD	Application	Ref.
1		Colorimetric & fluorescence	Turn-on	2.57 μM	Bioimaging	44
2		Colorimetric & ratiometric fluorescence	Turn-on	0.451 μM	Bioimaging	45
3		Fluorescence	Turn-off	0.47 μM	Logic gate & test kits	46
4		Fluorescence	Turn-on	4.92 μM	Bioimaging	47
5		Fluorescence	Turn-on	0.501 μM	Bioimaging & soil sample test	48
6		Fluorescence	Turn-off	4.68 μM	Real water sample test	49
7		Ratiometric fluorescence	Turn-off	2.91×10^{-5} M	—	50
8		Colorimetric & fluorescence	Turn-on	Colorimetric 7.83 μM Fluorometric 1.04 μM	Biological, logic gate & real sample tests	51
9		Colorimetric & fluorescence	Turn-off	1.87 μM	Real soil sample test	52
10		Colorimetric & fluorescence	Turn-off	Colorimetric 0.67 μM Fluorometric 0.24 μM	Real water analysis & test paper strips	This work
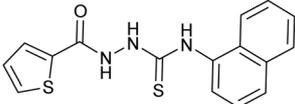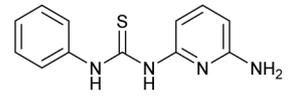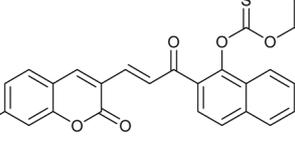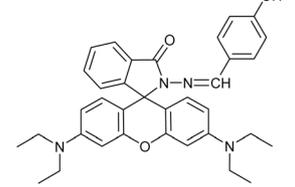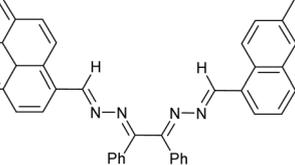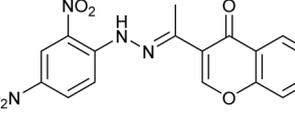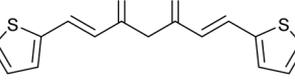
completed, which remained stable for up to 30 minutes as shown in Fig. 7a and b.

3.10 Density functional theory (DFT) calculations

The optimized geometry of TAA and TAA-Hg^{2+} complex through DFT is shown in (Fig. 8a and b). The TAA-Hg^{2+} complex, containing the Hg^{2+} metal centre, exhibits a tetrahedral geometry formed through coordination with a neutral ligand possessing an O_2 donor system of the TAA and two mononegative chloride counter ions, resulting in the formation of a mononuclear complex.

The theoretical evidence of the binding mechanism of TAA and Hg^{2+} was confirmed by DFT calculations with B3LYP/6-311G++ (d, p) as a basis set for the TAA probe and B3LYP/LANL2DZ basis set for the complex using the Gaussian 09 program.[42,43] As illustrated in (Fig. 8c) the frontier molecular orbitals of the TAA-Hg^{2+} complex are lower in energy ($\Delta E = 3.37$ eV) compared to the frontier molecular orbitals of the TAA probe alone ($\Delta E = 3.78$ eV). Thus, the complex is electronically more stable compared to the probe. The HOMO of the complex indicates that the probe significantly binds to the molecule with possible charge transfer between the metal ion and the probe upon excitation. This is a PET process, providing an explanation for the change in absorbance and fluorescence quenching.

3.11 pH studies

To evaluate the practical applicability of TAA in environmental and agricultural contexts, its fluorescence behaviour was analysed across a range of pH conditions with and without the Hg^{2+}. The solutions CH_3CN/H_2O (v/v, 1:1) were prepared with pH values ranging from 2 to 12 by gradually adding 1 M hydrochloric acid and 1 M sodium hydroxide, with pH monitored using a pH meter. As illustrated in Fig. 9, the fluorescence intensity of probe TAA remained stable between pH 2–9, but showed a gradual decline from pH 10–12, which was likely due to degradation of its molecular structure. The degradation of TAA structure in a basic medium is may be due to the nucleophilic attack by hydroxide ions leading to the cleavage of the heptadienone moiety, resulting in the loss of the active methylene group. Additionally, upon introducing Hg^{2+} to the TAA solution, there was a slight quenching in fluorescence intensity within the pH range of 2–6 in which the Hg^{2+} detection may not be significant. But at pH 7–9, significant fluorescence quenching was observed. Therefore, the optimal pH range for effective application of TAA for Hg^{2+} detection was between pH 7–9.

3.12 Reversibility of TAA

Reversibility and reusability are key attributes of an effective chemosensor. In this context, the reversible sensing ability of TAA was evaluated. Initially, TAA displayed an emission intensity at 505 nm. Upon the addition of Hg^{2+} ions, complete decrease in the fluorescence intensity was observed, indicating complex formation. To assess reversibility, a well-known chelating agent ethylenediaminetetraacetic acid (EDTA) (50 μM), was introduced to the TAA-Hg^{2+} complex (Scheme 2). Upon addition of EDTA, the fluorescence intensity was restored. This

fluorescence recovery confirmed the displacement of Hg^{2+} ions by EDTA, demonstrating the reversible binding interaction. Furthermore, this cycle of switching between fluorescence on–off was successfully repeated over 2 cycles with alternating additions of Hg^{2+} and EDTA (Fig. 10), affirming the ability of the TAA probe to reproduce and reuse.

4 Practical application

4.1 Real water sample analysis

To assess the practical utility of TAA for detecting Hg^{2+}, real-water sample experiments were conducted using five types of water: river water, pond water, distilled water, lake water and tap water from nearby places. Since these environmental samples were not fully purified, trace amounts of heavy metal ions could still be present. Using such water samples, Hg^{2+} detection is more challenging. Each sample was first filtered using Whatman filter paper. No significant fluorescence quenching was observed in the pretreated distilled water, tap water, pond water, lake water and river water samples, indicating minimal background interference. Subsequently, known concentrations of Hg^{2+} were introduced into each sample. Fluorescence intensity values were recorded and used to calculate Hg^{2+} concentrations using the linear calibration curve. The recovery rates of Hg^{2+}, shown in Table 2, ranged from 99.0% to 102.0%. These results clearly demonstrate the credibility and practical applicability of the TAA sensor for detecting Hg^{2+} in real environmental water samples.

4.2 Test strip analysis

Portable test strip-based detection provides a real-time, simple and efficient method for the visual recognition of target analytes. To evaluate the practical applicability of TAA, portable test strip experiments were carried out. Filter paper strips were coated with the solution of TAA (1 mM) and exposed to various
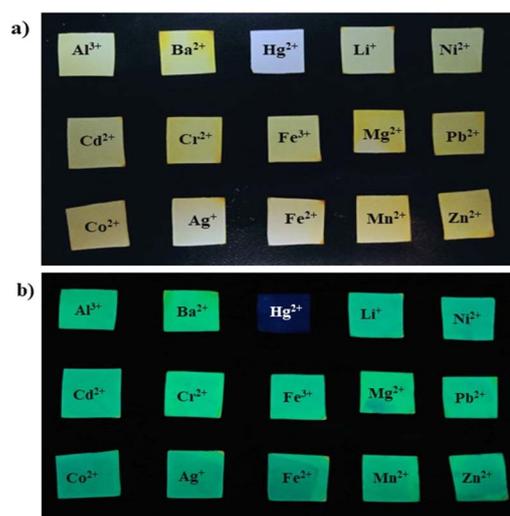

Fig. 11 TAA-coated (1 mM) test strips for Hg^{2+} (1 mM) in comparison with other metal ions: (a) visible light, (b) UV-light (365 nm).

metal ion solutions (1 mM) including Al^{3+}, Ba^{2+}, Cd^{2+}, Co^{2+}, Cr^{2+}, Ag^+, Fe^{3+}, Fe^{2+}, Hg^{2+}, Li^+, Mg^{2+}, Mn^{2+}, Ni^{2+}, Pb^{2+} and Zn^{2+}. In the visible light, all the test strips dipped in various metal ion solutions were yellow in color, except the one dipped in Hg^{2+} solution, which was colorless. This proves that TAA can be used as a naked eye sensor for Hg^{2+} detection using a test strip as a medium (Fig. 11a). Similarly, under 365 nm UV light, TAA exhibited a highly selective response to Hg^{2+} ions, evidenced by a clear quench in fluorescence. But not with other metal ions in the TAA-coated strips (Fig. 11b). These results demonstrate that TAA can function as a portable fluorometric sensor with excellent selectivity for the visual detection of Hg^{2+} ions.

5 Conclusion

We present an easy-to-use curcumin-based fluorescent probe (TAA) that functions as a colorimetric and fluorescence "turn-off" probe, demonstrating high sensitivity and selectivity for the detection of Hg^{2+} ions in a CH_3CN/H_2O (1 : 1, v/v) medium. The multifunctional sensing behaviour of TAA was confirmed by absorption and emission studies, which revealed hypsochromic shifts in absorption and quenching of emission intensity upon complexation with Hg^{2+}. In order to understand the sensitivity of TAA for Hg^{2+}, both absorption and emission studies were performed which revealed the colorimetric detection limit to be 0.67 μM and the fluorometric detection limit to be 0.24 μM. The Job's plot indicated 1 : 1 stoichiometry, and the B–H plot produced a binding affinity of 3.4×10^5 M^{-1}. The complex formation of Hg^{2+} onto TAA was confirmed by LC-MS, IR and DFT analysis. Nature of TAA and TAA-Hg^{2+} complex in different pH[2–12] was also studied, in which pH 7–9 was a suitable environment for Hg^{2+} detection. Reusability of TAA was studied using EDTA. Finally, the evident practicability of the TAA was validated through its high sensitivity in detecting low concentrations of Hg^{2+} in real water sample analysis. Its applicability on test strip applications and in the evaluation of various water samples highlights its exceptional property. The key attributes of TAA, such as reversibility, reusability, high selectivity, and practical applicability, highlight its significance in advancing colorimetric and fluorescent sensors for diverse analytical applications.

Data availability

The data supporting this article have been included as part of the ESI.†

Author contributions

Ramesh D. K.: conceptualization, methodology, investigation, visualization, writing – original draft, writing – review & editing. Prasad Pralhad Pujar: supervision, funding acquisition, writing – review & editing.

Conflicts of interest

There are no conflicts of interest to declare.

Acknowledgements

References

1 M. Medfu Tarekegn, Z. S. Fikirte and A. I. Ishetu, Microbes used as a tool for bioremediation of heavy metal from the environment, *Cogent Food Agric.*, 2020, **6**(1), 1783174, DOI: **10.1080/23311932.2020.1783174**.

2 J. Briffa, E. Sinagra and R. Blundell, Heavy metal pollution in the environment and their toxicological effects on humans, *Heliyon*, 2020, **6**(9), DOI: **10.1016/j.heliyon.2020.e04691**.

3 O. Dagdag, T. W. Quadri, R. Haldhar, S. C. Kim, W. Daoudi, E. Berdimurodov *et al.*, An Overview of Heavy Metal Pollution and Control, in *Heavy Metals in the Environment: Management Strategies for Global Pollution*, ACS Symposium Series, American Chemical Society, 2023, vol. 1456, pp. 3–24, DOI: **10.1021/bk-2023-1456.ch001**.

4 D. Paul, Research on heavy metal pollution of river Ganga: A review, *Ann. Agrar. Sci.*, 2017, **15**(2), 278–286. Available from: **https://www.sciencedirect.com/science/article/pii/S1512188716301142**.

5 S. Erdemir, S. Malkondu, M. Oguz and A. Kocak, Monitoring Hg2+ ions in food and environmental matrices using a novel ratiometric NIR fluorescent sensor via carbonothioate-deprotection reaction, *Environ. Pollut.*, 2024, **348**, 123859. Available from: **https://www.sciencedirect.com/science/article/pii/S0269749124005736**.

6 J. Chen, J. Tao, H. F. Yu, C. P. Ma, F. Tan and X. C. Wang, Highly selective chemosensor for the sensitive detection of Hg2+ in aqueous media and its cell imaging application, *Spectrochim. Acta, Part A*, 2023, **296**, 122648. Available from: **https://www.sciencedirect.com/science/article/pii/S1386142523003335**.

7 S. Seenan, S. Manickam and S. Kulathu Iyer, Fluorescent chemosensors for Hg2+ions based on a pyridine-attached phenanthridine probe, *New J. Chem.*, 2021, **45**(37), 17667–17673.

8 M. Kiani, M. Bagherzadeh, S. Meghdadi, N. Rabiee, A. Abbasi, K. Schenk-Joß, *et al.*, Development of a novel carboxamide-based off–on switch fluorescence sensor: Hg2+, Zn2+ and Cd2+, *New J. Chem.*, 2020, **44**(27), 11841–11852, DOI: **10.1039/D0NJ02595J**.

9 X. Guo, X. Qian and L. Jia, A Highly Selective and Sensitive Fluorescent Chemosensor for Hg2+ in Neutral Buffer Aqueous Solution, *J. Am. Chem. Soc.*, 2004, **126**(8), 2272–2273, DOI: **10.1021/ja037604y**.

10 A. Kumar, V. Kumar and K. K. Upadhyay, A ninhydrin based colorimetric molecular switch for Hg2+ and CH3COO−/F−, *Tetrahedron Lett.*, 2011, **52**(50), 6809–6813. Available from: **https://www.sciencedirect.com/science/article/pii/S0040403911017679**.

11 Y. Gao, S. De Galan, A. De Brauwere, W. Baeyens and M. Leermakers, Mercury speciation in hair by headspace

injection–gas chromatography–atomic fluorescence spectrometry (methylmercury) and combustion-atomic absorption spectrometry (total Hg), *Talanta*, 2010, **82**(5), 1919–1923. Available from: https://www.sciencedirect.com/science/article/pii/S0039914010006296.

12 F. Moreno, T. García-Barrera and J. L. Gómez-Ariza, Simultaneous analysis of mercury and selenium species including chiral forms of selenomethionine in human urine and serum by HPLC column-switching coupled to ICP-MS, *Analyst*, 2010, **135**(10), 2700–2705.

13 E. J. Arar and J. D. Pfaff, Determination of dissolved hexavalent chromium in industrial wastewater effluents by ion chromatography and post-column derivatization with diphenylcarbazide, *J. Chromatogr. A*, 1991, **546**, 335–340. Available from: https://www.sciencedirect.com/science/article/pii/S0021967301930316.

14 K. Yin, F. Yu, D. Liu, Z. Xie and L. Chen, Cyanine-based colorimetric and fluorescent probe for the selective detection of diethylstilbestrol in seawater, shrimp and fish samples, *Sens. Actuators, B*, 2016, **223**, 799–805. Available from: https://www.sciencedirect.com/science/article/pii/S0925400515304809.

15 D. Dai, Z. Li, J. Yang, C. Wang, J. R. Wu, Y. Wang, *et al.*, Supramolecular Assembly-Induced Emission Enhancement for Efficient Mercury(II) Detection and Removal, *J. Am. Chem. Soc.*, 2019, **141**(11), 4756–4763, DOI: 10.1021/jacs.9b01546.

16 M. H. Lee, J. S. Wu, J. W. Lee, J. H. Jung and J. S. Kim, Highly Sensitive and Selective Chemosensor for Hg2+ Based on the Rhodamine Fluorophore, *Org. Lett.*, 2007, **9**(13), 2501–2504, DOI: 10.1021/ol0708931.

17 H. Dai, Y. Yan, Y. Guo, L. Fan, Z. Che and H. Xu, A Selective and Sensitive "Turn-on" Fluorescent Chemosensor for Recognition of Hg2+ Ions in Water, *Chem.–Eur. J.*, 2012, **18**(36), 11188–11191, DOI: 10.1002/chem.201201604.

18 X. Cheng, Q. Li, C. Li, J. Qin and Z. Li, Azobenzene-Based Colorimetric Chemosensors for Rapid Naked-Eye Detection of Mercury(II), *Chem.–Eur. J.*, 2011, **17**(26), 7276–7281, DOI: 10.1002/chem.201003275.

19 J. Wang, Q. Rao, H. Wang, Q. Zhang, G. Liu, Z. Wu, *et al.*, A terpyridine-based test strip for the detection of Hg 2+ in various water samples and drinks, *Anal. Methods*, 2019, **11**(2), 227–231.

20 Y. Huo, S. Wang, T. Lu, C. Pan, Y. Lu, X. Yang, *et al.*, Highly selective and sensitive colorimetric chemosensors for Hg2+ based on novel diaminomaleonitrile derivatives, *RSC Adv.*, 2016, **6**(7), 5503–5511.

21 H. Mohammad, A. S. M. Islam, C. Prodhan and M. Ali, A fluorescein-based chemosensor for "turn-on" detection of Hg2+ and the resultant complex as a fluorescent sensor for S2− in semi-aqueous medium with cell-imaging application: experimental and computational studies, *New J. Chem.*, 2019, **43**(14), 5297–5307.

22 B. D. Vanjare, P. G. Mahajan, H. I. Ryoo, N. C. Dige, N. G. Choi, Y. Han, *et al.*, Novel rhodamine based chemosensor for detection of Hg2+: Nanomolar detection, real water sample analysis, and intracellular cell imaging,

23 *Sens. Actuators, B*, 2021, **330**, 129308. Available from: https://www.sciencedirect.com/science/article/pii/S0925400520316488.

23 E. G. Cansu Ergun, G. Ertas and D. Eroglu, A benzimidazole-based turn-off fluorescent sensor for selective detection of mercury (II), *J. Photochem. Photobiol., A*, 2020, **394**, 112469. Available from: https://www.sciencedirect.com/science/article/pii/S1010603020302689.

24 P. C. ayya swamy, J. Shanmugapriya, S. Singaravadivel, G. Sivaraman and D. Chellappa, Anthracene-Based Highly Selective and Sensitive Fluorescent "Turn-on" Chemodosimeter for Hg2+, *ACS Omega*, 2018, **3**(10), 12341–12348, DOI: 10.1021/acsomega.8b01142.

25 B. M. Chethanakumar, K. B. Gudasi, R. S. Vadavi and S. S. Bhat, Luminescent Pyrene-based Schiff base Receptor for Hazardous Mercury(II) Detection Demonstrated by Cell Imaging and Test Strip, *J. Fluoresc.*, 2023, **33**(2), 539–551, DOI: 10.1007/s10895-022-03066-2.

26 J. M. V. Ngororabanga, Z. R. Tshentu and N. Mama, A New Highly Selective Colorimetric and Fluorometric Coumarin-based Chemosensor for Hg2+, *J. Fluoresc.*, 2020, **30**(5), 985–997, DOI: 10.1007/s10895-020-02542-x.

27 S. Vishnu, S. Maity, A. C. Maity, M. S. Kumar, M. Dolai, A. Nag, *et al.*, Development of a fluorescent scaffold by utilizing quercetin template for selective detection of Hg2+: Experimental and theoretical studies along with live cell imaging, *Spectrochim. Acta, Part A*, 2024, **5**, 315.

28 V. Sharma, S. Dutta, R. K. Roy, S. Manna, S. M. Choudhury and G. K. Patra, Highly sensitive benzildihydrazone-N,N'-bis(2-hydroxy-4-diethylamino-1-formylbenzene) stabilized ZnS nanoparticles as potential optical chemosensors for Hg2+ ions: Anticancer activity and biosensor imaging, *J. Mol. Struct.*, 2025, **1329**, 141398. Available from: https://www.sciencedirect.com/science/article/pii/S0022286025000870.

29 N. Horzum, D. Mete, E. Karakuş, M. Üçüncü, M. Emrullahoğlu and M. M. Demir, Rhodamine-Immobilised Electrospun Chitosan Nanofibrous Material as a Fluorescence Turn-On Hg2+ Sensor, *ChemistrySelect*, 2016, **1**(5), 896–900, DOI: 10.1002/slct.201600027.

30 N. Ghalandarlaki, A. M. Alizadeh and S. Ashkani-Esfahani, Nanotechnology-Applied Curcumin for Different Diseases Therapy, *BioMed Res. Int.*, 2014, **2014**(1), 394264, DOI: 10.1155/2014/394264.

31 A. K. Panda, C. Dwaipayan, S. Irene, K. Tila and G. Sa, New insights into therapeutic activity and anticancer properties of curcumin, *J. Exp. Pharmacol.*, 2017, **9**, 31–45, DOI: 10.2147/JEP.S70568.

32 T. Esatbeyoglu, P. Huebbe, I. M. A. Ernst, D. Chin, A. E. Wagner and G. Rimbach, Curcumin—From Molecule to Biological Function, *Angew. Chem., Int. Ed.*, 2012, **51**(22), 5308–5332, DOI: 10.1002/anie.201107724.

33 R. Carolina Alves, P. F. Richard, F. S. Bruno, D. V. Francesca and M. Chorilli, A Critical Review of the Properties and Analytical Methods for the Determination of Curcumin in Biological and Pharmaceutical Matrices, *Crit. Rev. Anal.*

Chem., 2019, **49**(2), 138–149, DOI: **10.1080/10408347.2018.1489216**.

34 X. Lan, Y. Liu, L. Wang, H. Wang, Z. Hu, H. Dong, *et al.*, A review of curcumin in food preservation: Delivery system and photosensitization, *Food Chem.*, 2023, **424**, 136464. Available from: **https://www.sciencedirect.com/science/article/pii/S0308814623010828**.

35 K. Mahmood, K. M. Zia, M. Zuber, M. Salman and M. N. Anjum, Recent developments in curcumin and curcumin based polymeric materials for biomedical applications: A review, *Int. J. Biol. Macromol.*, 2015, **81**, 877–890. Available from: **https://www.sciencedirect.com/science/article/pii/S0141813015006418**.

36 S. N. Margar, L. Rhyman, P. Ramasami and N. Sekar, Fluorescent difluoroboron-curcumin analogs: An investigation of the electronic structures and photophysical properties, *Spectrochim. Acta, Part A*, 2016, **152**, 241–251. Available from: **https://www.sciencedirect.com/science/article/pii/S138614251530113X**.

37 H. Cho, J. B. Chae and C. Kim, A thiophene-based blue-fluorescent emitting chemosensor for detecting indium (III) ion, *Inorg. Chem. Commun.*, 2018, **97**, 171–175.

38 A. N. Nurfina, M. S. Reksohadiprodjo, H. Timmerman, U. A. Jenie, D. Sugiyanto and H. van der Goot, Synthesis of some symmetrical curcumin derivatives and their antiinflammatory activity, *Eur. J. Med. Chem.*, 1997, **32**(4), 321–328. Available from: **https://www.sciencedirect.com/science/article/pii/S0223523497890848**.

39 R. Hemmati, A. Abdi, M. Feizi-Dehnayebi, M. Farajzadeh, G. M. Ziarani, A. Banitalebi, *et al.*, Benzoguanamine dimer as a novel fluorophore probe for Hg2+ ion detection in Pampus argenteus fish supported by DFT approach, *J. Environ. Chem. Eng.*, 2025, 116981. Available from: **https://www.sciencedirect.com/science/article/pii/S221334372501677X**.

40 M. A. Kamyabi, D. Kazemi, R. Bikas and F. Soleymani-Bonoti, Investigation of the Hg(II) biosorption from wastewater by using garlic plant and differential pulse voltammetry, *Anal. Biochem.*, 2021, **627**, 114263. Available from: **https://www.sciencedirect.com/science/article/pii/S0003269721001640**.

41 R. Bhaskar and S. Sarveswari, Thiocarbohydrazide based Schiff Base as a Selective Colorimetric and Fluorescent Chemosensor for Hg2+ with "Turn-Off" Fluorescence Responses, *ChemistrySelect*, 2020, **5**(13), 4050–4057, DOI: **10.1002/slct.202000652**.

42 J. E. Del Bene, W. B. Person and K. Szczepaniak, Properties of Hydrogen-Bonded Complexes Obtained from the B3LYP Functional with 6-31G(d,p) and 6-31+G(d, p) Basis Sets: Comparison with MP2/6-31+G(d, p) Results and Experimental Data, *J. Phys. Chem.*, 1995, **99**(27), 10705–10707, DOI: **10.1021/j100027a005**.

43 H. Kruse, L. Goerigk and S. Grimme, Why the Standard B3LYP/6-31G* Model Chemistry Should Not Be Used in DFT Calculations of Molecular Thermochemistry: Understanding and Correcting the Problem, *J. Org. Chem.*, 2012, **77**(23), 10824–10834, DOI: **10.1021/jo302156p**.

44 B. U. Gauthama, B. Narayana, B. K. Sarojini, N. K. Suresh, Y. Sangappa, A. K. Kudva, *et al.*, Colorimetric "off–on" fluorescent probe for selective detection of toxic Hg2+ based on rhodamine and its application for in-vivo bioimaging, *Microchem. J.*, 2021, **166**, 106233.

45 P. Ravichandiran, V. K. Kaliannagounder, N. Maroli, A. Boguszewska-Czubara, M. Masłyk, A. R. Kim, *et al.*, A dual-channel colorimetric and ratiometric fluorescence chemosensor for detection of Hg2+ ion and its bioimaging applications, *Spectrochim. Acta, Part A*, 2021, **257**, 119776.

46 W. L. Guan, Y. F. Zhang, Q. P. Zhang, Y. M. Zhang, T. B. Wei, H. Yao, *et al.*, A novel fluorescent chemosensor based on naphthofuran functionalized naphthalimide for highly selective and sensitive detecting Hg2+ and CN, *J. Lumin.*, 2022, **244**, 118722. Available from: **https://www.sciencedirect.com/science/article/pii/S0022231321008383**.

47 H. Kim, M. Lee, J. J. Lee, E. K. Min, K. T. Kim and C. Kim, A solvent-dependent dual chemosensor for detecting Zn2+ and Hg2+ based on thiophene and thiourea functional groups by fluorescence turn-on, *J. Photochem. Photobiol., A*, 2022, **428**, 113882. Available from: **https://www.sciencedirect.com/science/article/pii/S1010603022001113**.

48 P. Mohanty, P. P. Dash, S. Naik, R. Behura, M. Mishra, H. Sahoo, *et al.*, A thiourea-based fluorescent turn-on chemosensor for detecting Hg2+, Ag+ and Au3+ in aqueous medium, *J. Photochem. Photobiol., A*, 2023, **437**, 114491. Available from: **https://www.sciencedirect.com/science/article/pii/S1010603022007146**.

49 H. Li, J. Yan, L. Jiang, Y. Zhao, Y. Song, J. Yu, *et al.*, Selective and Sensitive Detection of Hg2+ and Ag+ by a Fluorescent and Colorimetric Probe with Large Stokes Shift, *J. Fluoresc.*, 2023, **34**, 2793–2806.

50 S. S. Dash, P. Mohanty, P. K. Kar and R. Bhaskaran, A Novel Rhodamine Functionalized Schiff Base Type Ratiometric Fluorescent Chemosensor for the Sensing of Hg2+ Ions; Experimental and Theoretical Approach, *J. Fluoresc.*, 2025, DOI: **10.1007/s10895-024-04132-7**.

51 A. Pandey, D. Kumar, S. Dutta, S. Manna, S. M. Choudhury, V. Sharma, *et al.*, A pyrene based novel di-Schiff base colorimetric and turn-on fluorescent-chemosensor for selective and sensitive detection of Hg2+ ion: Biological, logic gate and real sample applications, *Spectrochim. Acta, Part A*, 2025, **337**, 126104. Available from: **https://www.sciencedirect.com/science/article/pii/S138614252500410X**.

52 S. R. Kar, P. P. Dash, S. N. Panda, P. Mohanty, D. Mohanty, A. K. Barick, *et al.*, A Formyl Chromone Based Schiff Base Derivative: An Efficient Colorimetric and Fluorescence Chemosensor for the Selective Detection of Hg2+ Ions, *J. Fluoresc.*, 2023, **35**, 483–495.